## **METHOD**

The purpose of the test was to evaluate concepts for delivery of the seismic sensors via the completion tubing. Key criteria were (1) the coupling of the sensors to the formation, (2) S/N for the different systems, and (3) performance of the fiberoptic sensors relative to reference VSP tool measurements.

Two systems were evaluated. The first system is a passive seismic mandrel (PSM) (Figure 7, left). This system simply re-

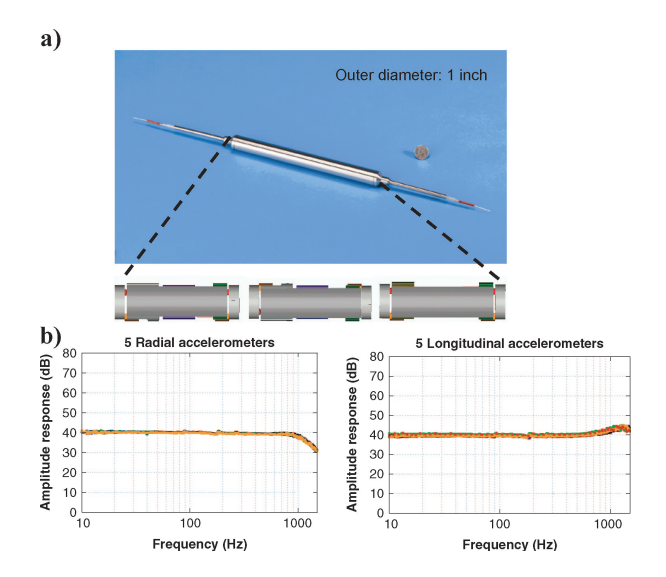


Figure 6. (a) A 3C-accelerometer package with three sensor orientations. (b) Nominal frequency responses of the two accelerometer types with each plot containing responses of five individual sensors of the same type (Knudsen et al., 2003).

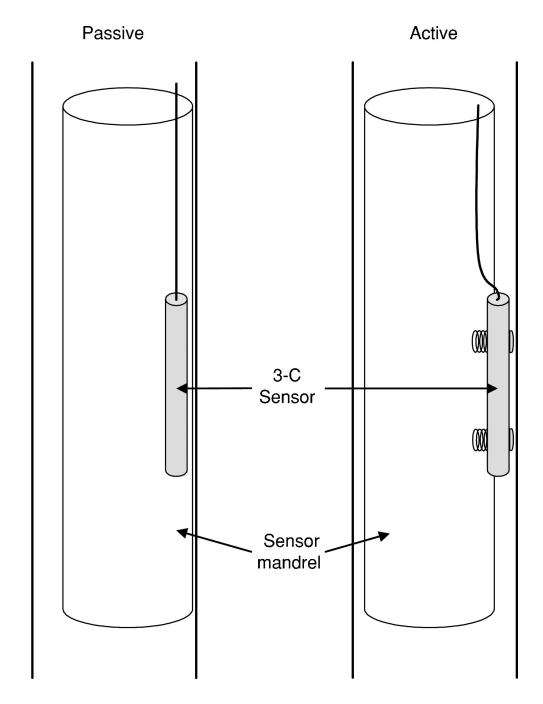


Figure 7. Coupling systems. (Left) PSM design relies on the weight of the production tubing for coupling. (Right). ASC uses a spring-loaded pad device to achieve a coupling force and decouple the sensors from the tubing resonances.

lies on the weight of the production tubing to couple the 3C sensors to the borehole wall. The second system is an active seismic clamp (ASC). This type of system uses a spring-loaded pad to couple the sensors to the borehole wall and to help isolate the sensors from tubing resonances (Figure 7, right).

For well completion purposes, the PSM is desirable due to its simple design and lack of moving parts. On the other hand, the ASC design may be required to achieve an adequate S/N for recording seismic signals reflected off of bedding features. It also is advantageous for nondeviated wells.

The design objectives for the passive seismic mandrel were natural coupling through gravitational and tubing/casing forces, an outside diameter of the mandrel slightly less than the inside diameter of the casing, total package as short and stiff as possible to minimize resonance behavior, no moving parts, minimal number of parts, flutes/slots to allow bypass fluid flow, clamp-on or threaded mandrel style, and separate sensor subassembly.

In Figure 8 are shown the final PSM and ASC prototypes prior to installation in the well. The PSM prototype device (Figure 8, left) takes all of the design objectives into consideration. A threaded mandrel was ultimately chosen for minimizing production-well deployment risk. The optimal mandrel shape was determined to be tubular, concentric to the borehole. In contrast, the ASC was designed to house the 3C fiber-optic accelerometers in a clamp-on device, similar to a cable protector. The design uses a spring-loaded pad to couple the sensor package to the casing, isolating as much as possible the three accelerometers from the clamp, tubing, and the connected fiber optic cable (Figure 8, right).

## FIELD TEST

The Rocky Mountain Oilfield Testing Center (RMOTC) was chosen as the test site. Conditions at RMOTC were favorable for rapid drilling and well completion and broad access for seismic-energy-source deployment.



Figure 8. (Left) Final PSM prototype. A threaded mandrel was ultimately chosen for minimizing production-well deployment risk. The optimal mandrel shape was determined to be tubular, concentric to the borehole. (Right) Final ASC prototype, designed to house the 3C fiber-optic accelerometers in a clamp-on device, similar to a cable protector. The design uses a spring-loaded pad to couple the sensor package to the casing, isolating as much as possible the three accelerometers from the clamp, tubing, and the connected fiber-optic cable.

An inclined wellbore with a 7-in, 23-lb casing was drilled to a total depth of 395 m with very few operational problems (Figure 9). The DOE  $13 \times 23$  well was drilled, cased, cemented, and logged over the period May 8 through May 21, 2002. The well achieved the field-test objectives by reaching a well deviation of more than  $40^{\circ}$  in as shallow a well as possible. A single string of casing was used beyond the surface conductor. Good cement bond was attained up to approximately 90-m measured depth (MD). Although this did not allow for testing tool coupling in a straight wellbore section, testing was possible to within approximately  $3^{\circ}$  of vertical. The purpose-drilled well allowed for testing of both the passive and active devices.

In order to evaluate the feasibility of the two deployment approaches to detect seismic signals over an acceptable range of hole deviations, the test plan included conducting vertical incidence (walkover) and fixed-offset VSP surveys, walkaway lines, and various single-point offset shooting. Both vibrator and dynamite shot-hole energy sources were employed. Performance characteristics, including amplitude, S/N, resonance, dynamic range, and directionality, were evaluated. Figure 10

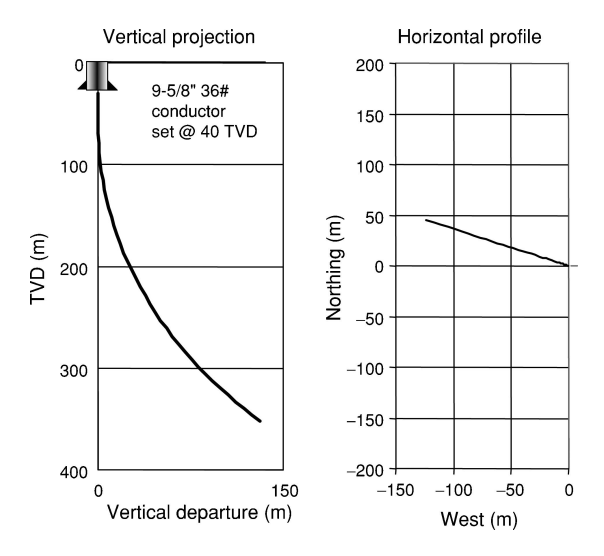


Figure 9. Directional survey. The well was drilled to a depth of 408 m (364 m TVD) and with a maximum deviation of 40°.

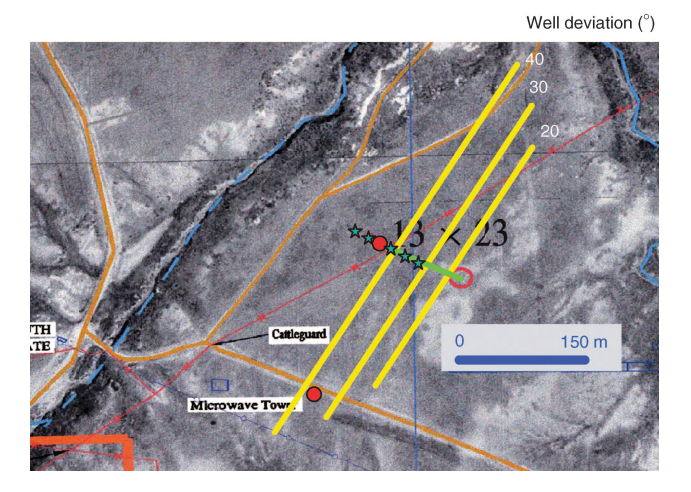


Figure 10. Location of walkaway surveys (yellow lines) and fixed-offset source positions (green stars).

shows the location of walkaway surveys (yellow lines) and fixed-offset source positions (green stars).

In order to acquire the fiber-optic VSP data, the tubing-conveyed, single-station 3C sensors were deployed at various depths, much like a wireline operation. The significant difference was that the sensors were positioned using pipe tallying, essentially keeping track of the pipe joint lengths (whole length or fraction thereof) to determine the position of the sensor station in the well. For the walkaway lines, the conventional slim VSP receiver was positioned inside the tubing at the same depth as the fiber-optic sensors (Figure 11). Accurate depth positioning was determined using a collar locator (CCL)

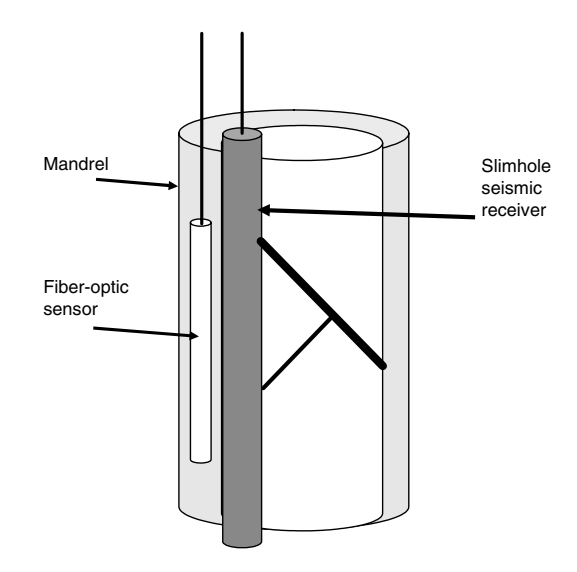


Figure 11. Schematic of the permanent fiber-optic and reference electrical-wireline procedure. At each station, the wireline VSP was positioned in the tubing behind the fiber-optic sensor, and data were acquired simultaneously with both sets of sensors.

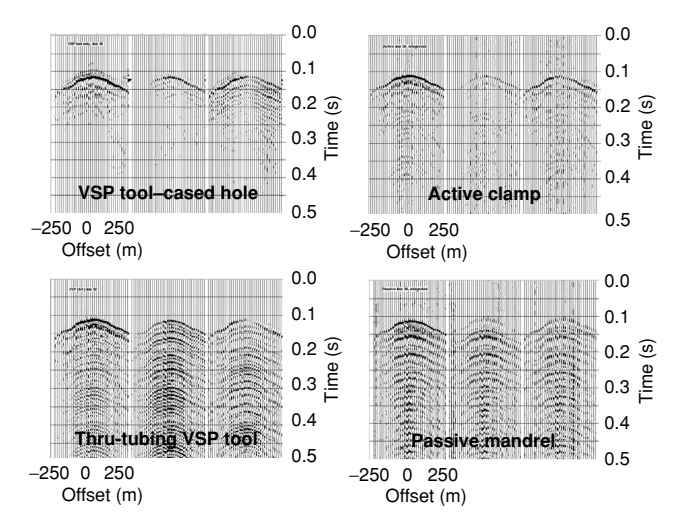


Figure 12. Walkaway VSP measurements for both activeclamp and passive-mandrel sensors compared to the reference wireline VSP data acquired in the cased hole and through the tubing during the fiber-optic sensor measurements. Each set of three plots contains shows axial and two orthogonal radial components; the wellbore deviation is 30°. Fiber-optic accelerometer data are integrated for direct comparison with the VSP geophone data.

E16 Hornby et al.

device attached to the VSP tool. For the same lines, the fiber-optic sensor orientation was directly determined using a gyro tool temporarily lowered inside the tubing close to the sensor mandrel. A keyed sub located below the seismic sensor assembly allowed the gyro tool to accurately determine the "tool-face" of the fiber-optic sensor package. Optical sensor data were output in analog electronic form to a conventional seismic recording system employing dedicated VSP-acquisition and quality-control software. All comparison data (shown

in Figure 12) were generated using a single vibrator with a 12–200 Hz sweep.

Three-component data from a walkaway line are shown for the various sensor configurations in Figure 12. Each set of three plots shows axial and two orthogonal radial components; the wellbore angle is 30°. For comparison purposes with the geophone data, the accelerometer data are integrated. In general, the PSM-deployed fiber-optic sensors acquired data with quality and characteristics equivalent to the

thru-tubing VSP tool with conventional geophones. Both contain a significant amount of reverberations interpreted to be pipe modes and tube waves. The ASC-deployed fiber-optic sensors data contain significantly reduced ringing modes and compares more directly to the empty cased-hole deployed VSP tool.

Both the PSM- and the ASC-deployed sensors exhibited good directional response. Direct-arrival hodograms from both the ASC and the PSM data track the source as it traverses a walkaway line (Figure 13). The ASC sensor hodograms, however, are more linear in character, suggesting superior S/N response.

Figure 14 shows a series of plots of fixed-offset surveys comparing the casedhole wireline VSP with the fiber-optic sensor data acquired with the ASC and PSM for a fixed-offset survey with a source position 137 m from the wellhead. Axial components are shown for all data. Data from the ASC best matches the VSP tool, whereas the PSM data exhibits both resonances in the direct P-wave signal and tube-wave-related noise. Fiber-optic accelerometer data are integrated for direct comparison with the VSP geophone data. Figure 15 shows axial components of wireline VSP and integrated fiberoptic accelerometer data with ASC for a source position 198 m from the wellhead. A good match between the integrated fiber-optic and wireline-geophone data is seen, particularly for the strong upgoing arrival that intersects the y-axis around 0.15 s. Figure 16 shows spectral analysis of S/N using the multiple coherency function (White 1973). This method attempts to analyze coherent signals versus incoherent noise. This figure was generated using a 350-ms time window centered at 175 ms. A total of 47 traces and a rolling buffer of 4 traces were used for the analysis. For the standard VSP sensor, we see a bandwidth of around 20 to 130 Hz; for the fiber-optic sensor, a slightly wider bandwidth of around 10 to 140 Hz is seen. Both data sets have about 15-dB gain of coherent signal over noise. We conclude that

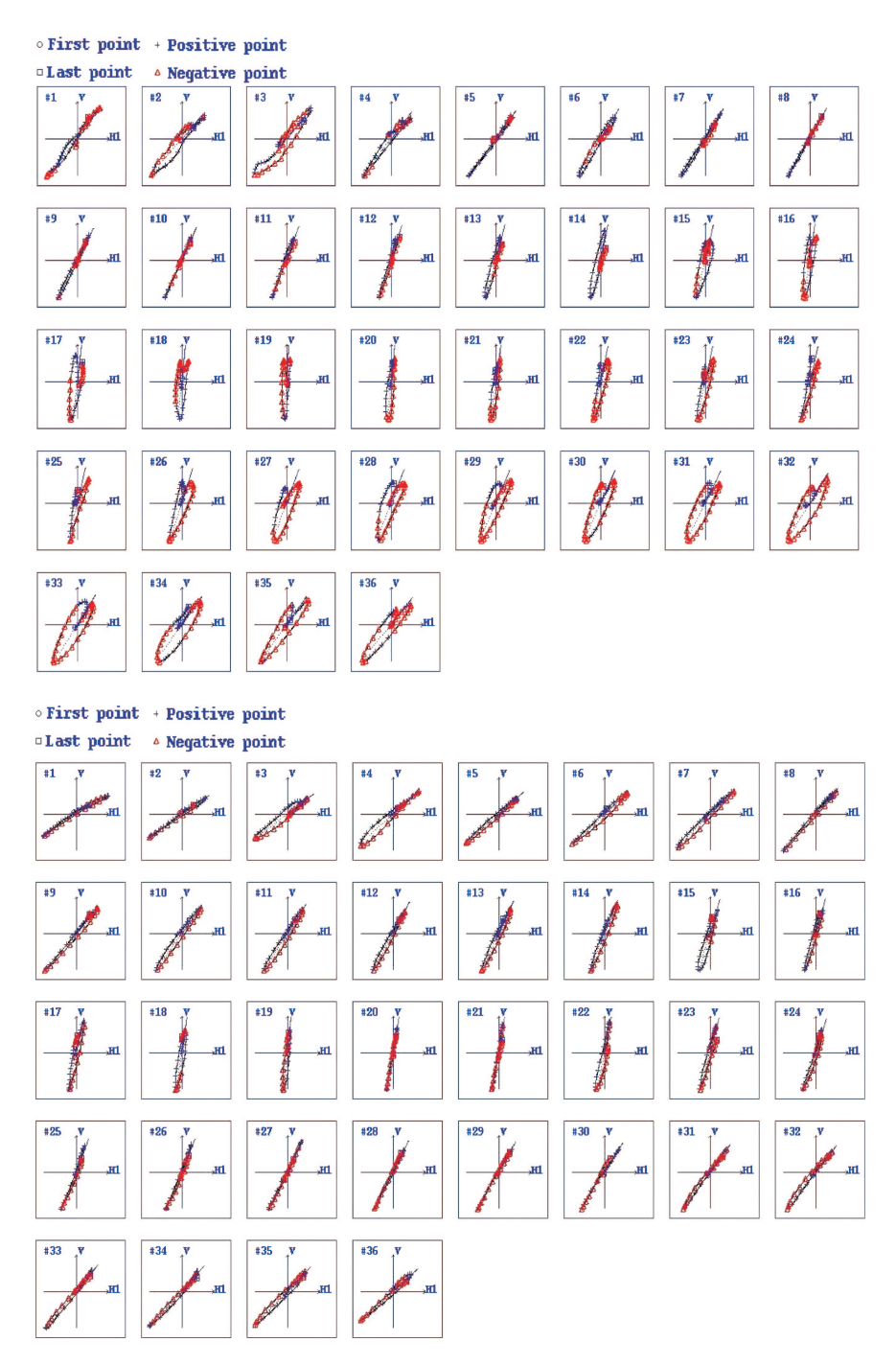


Figure 13. Hodograms from both the ASC (bottom) and PSM (top) show good tracking of the source as it traverses a walkaway line.